

1/5/78
30
6/5/78

BNL- 23844
OG-375
INFORMAL REPORT

MASTER

A Compilation of Invariant Cross Sections for the Reactions

π^\pm , K^\pm and $p^\pm + p \rightarrow \pi^0 + X$ at 100, 200 and 300 GeV/c

G. Donaldson, H.A. Gordon, K.-W. Lai, and I. Stumer
Brookhaven National Laboratory, Upton, New York 11973

A.V. Barnes, D. J. Mellema,^{b)} A.V. Tollestrup,^{a)} and R. L. Walker
California Institute of Technology, Pasadena, California 91125

and

O.I. Dahl, R.A. Johnson,^{c)} A. Ogawa, M. Pripstein, and S. Shannon
Lawrence Berkeley Laboratory, Berkeley, California 94720

- a) Present address: Fermi National Accelerator Laboratory, P.O. Box 500, Batavia, Illinois 60510.
- b) Present address: Hughes Aircraft Company, Culver City, California 90230
- c) Present address: Brookhaven National Laboratory, Upton, New York 11973

CONFIDENTIAL
This document contains neither recommendations nor conclusions of the Energy Research and Development Administration or the Department of Energy. It has been approved for public release and unlimited distribution. Its contents do not necessarily reflect official views of the Energy Research and Development Administration or the Department of Energy, and the Energy Research and Development Administration or the Department of Energy does not assume responsibility for use of the contents by other than intended recipients.

1/5/78

BNL - 23844
OG-375
INFORMAL REPORT

A Compilation of Invariant Cross Sections for the Reactions

π^\pm , K^\pm and $p^\pm + p \rightarrow \pi^0 + X$ at 100, 200 and 300 GeV/c

G. Donaldson, H.A. Gordon, K.-W. Lai, and I. Stumer
Brookhaven National Laboratory, Upton, New York 11973

A.V. Barnes, D. J. Mellema,^{b)} A.V. Tollestrup,^{a)} and R. L. Walker
California Institute of Technology, Pasadena, California 91125

and

O.I. Dahl, R.A. Johnson,^{c)} A. Ogawa, M. Pripstein, and S. Shannon
Lawrence Berkeley Laboratory, Berkeley, California 94720

We present measurements of the invariant cross section for various beam species to produce π^0 mesons at high transverse momentum in the reaction beam + proton $\rightarrow \pi^0 + \text{anything}$. These measurements were taken at Fermilab at 100, 200 and 300 GeV/c.

a) Present address: Fermi National Accelerator Laboratory, P.O. Box 500, Batavia, Illinois 60510.

b) Present address: Hughes Aircraft Company, Culver City, California 90230

c) Present address: Brookhaven National Laboratory, Upton, New York 11973

This publication is intended to supplement articles appearing elsewhere, in which insufficient space existed for a tabular presentation of data. To this end, no discussion of detection or analysis techniques appears, however, a brief description of the experiment will serve to elucidate the references wherein more thorough discussions of the apparatus and physics topics have been given. The experiment was conducted in 1974-1976 in the M2 beam line at FNAL, where it followed the original "charge exchange" experiment measuring differential cross sections for the reactions $\pi^- p \rightarrow \pi^0 n$ and $\pi^- p \rightarrow \eta^0 n$.⁽¹⁻⁴⁾ The apparatus consisted of two independent differential Cerenkov counters for tagging beam particles, a 60 cm liquid hydrogen target, and a Pb-scintillator sandwich photon detector. The detector generated a trigger whenever the transverse momentum (p_{\perp}) of the detected photons exceeded a preset value, and the angular acceptance was varied by arranging the position of the photon detector relative to the target. The production of π^0 and η^0 mesons has been discussed in several references.⁽⁵⁻⁸⁾ The data were taken in three broad angular regions: "90°" (43° - 115° center of mass [c.m.]), "30°" (15° - 52° c.m.), and "10°" (2° - 20° c.m.).

The position and energy of showers found in the detector allowed the mass of the parent particle to be reconstructed. To determine the invariant cross sections, we extracted the number of π^0 's (n_{π^0}) from the mass spectra of photon pairs (corrected for geometrical acceptance and with empty target background subtracted). The cross section was then computed by summing the events in bins of p_{\perp} and $x_{||}$ according to the formula

$$\frac{E}{dp} \frac{d\sigma}{dp^3} = \left(\frac{1}{2\pi p_{\max}} \right) \cdot \left(\frac{\Delta}{\rho l} \right) \cdot \frac{1}{\Phi.f_{\pi,K,p}} \cdot \frac{n_{\pi^0}}{dx_{||} dp_{\perp}}$$

where $n_\pi = \sum$ events $\frac{E^*}{p_\perp \cdot \epsilon}$ and E^* = energy of π^0 in the beam-target c.m. system
 p_\perp = transverse momentum of π^0
 ϵ = monte carlo geometrical efficiency
(at these values of p_\perp and $x_{||} = (p_{||}/p_{\max})$ c.m.)

and

$$\left(\frac{A}{\rho L}\right) = 4.0 \times 10^{-25} \text{ target factor involving target density, length, and Avogadro's number}$$

p_{\max} = maximum c. m. momentum

$\dot{\phi}$ = flux of incident particles (corrected for contamination due to electrons and misidentified particles)

$f_{\pi, K, p}$ = fraction of beam having Cerenkov counters' signature taken to be π , K , or proton, respectively.

$dx_{||} dp_\perp$ = bin size in $x_{||}$, p_\perp .

Beam compositions were determined by accepting Cerenkov signatures in which both counters unambiguously identified the beam particle. Under certain running conditions contaminations existed within a particular signature, however the known contaminations (shown in Table I) have been removed from the cross sections.

The measurements were taken at several p_\perp biases at each region of angular acceptance, and for various running periods we employed several different operating conditions for the Cerenkov counter and photon detector. Much could be said concerning possible systematic effects between the many data sets, however this requires a fuller discussion than is intended herein, and the values appearing in these tables are computed using only the measured fluxes. As an indication of the expected magnitude of such uncertainties, we have included a 14% point to point "floor" for the uncertainties of each cross section. When the statistical uncertainty exceeds this value, only the statistical uncertainty appears. Not included in the point to point uncertainty is an additional 5% uncertainty in normalization, and an uncertainty of 3% in the p_\perp scale.

The data are presented as follows: Figure 1 shows the regions of geometrical acceptance, and where measurements exist. Following are several tables giving the invariant cross section (in bins of p_{\perp} , $x_{||}$) for several incident beams. The small flux of K^+ and \bar{p} requires the widest possible $x_{||}$ bins to be used, and for comparison π^{\pm} , and p cross sections are also given in the same intervals. Finally, a series of figures showing the invariant cross section (for certain p_{\perp} intervals) is plotted against $x_{||}$, and again against $\theta_{c.m.}$. For the $\theta_{c.m.}$ plots, the data are plotted at the $\theta_{c.m.}$ corresponding to the center and width of a p_{\perp} , $x_{||}$ bin, i.e. the events are not re-histogrammed. The smooth curves on the plots serve to guide the eye, and are the result of a global least squares fit to data for each beam type at all available energies to the form

$$E \frac{dc}{d^3 p} = \frac{A * (1-x_D)^F}{(p_{\perp}^2 + m^2)^N}$$

where $x_D = \left\{ x_{\perp}^2 + (x_{||} - x_0)^2 \right\}^{1/2}$ and $x_{\perp} = (p_{\perp}/p_{\max})_{c.m.}$. The optimum values of the parameters A , m^2 , F , N and x_0 are determined from the fit and are given in Table I. Note that x_0 allows the $x_{||}$ distribution to reach a maximum at $x \neq 0$, and if $x_0 = 0$, x_D reduces to the familiar $x_R = (x_{\perp}^2 + x_{||}^2)^{1/2}$. The interpretation of this parameterization is the subject of Ref. 6.

In conclusion, this report is intended to present the primary measurements of the experiment (without interpretation or discussion) which are unfortunately too extensive to be published rapidly. Thus, the material of topical interest may be made available immediately to the scientists in this field for whom the accurate values of the cross sections may be of interest.

REFERENCES

1. A. V. Barnes et al., Phys. Rev. Lett. 37, 76 (1976).
2. O. I. Dahl et al., Phys. Rev. Lett. 37, 80 (1976).
3. O. I. Dahl et al., Phys. Rev. Lett. 38, -4 (1977).
4. R. A. Johnson, "Measurement of the $\pi^- p \rightarrow \pi^0 n$ and $\pi^- p \rightarrow \eta n$ Differential Cross Sections at Beam Momenta from 20 to 200 GeV/c", Ph.D. Thesis, UCBL-4610, (1975).
5. G. Donaldson et al., Phys. Rev. Lett. 36, 1110 (1976).
6. G. Donaldson et al., "Angular Dependence of High Transverse Momentum Inclusive π^0 Production in $\pi^- p$ and $p\bar{p}$ Interactions", BNL-23088-R.
7. G. Donaldson, et al., "A Comparison of High Transverse Momentum π^0 Production from π^\pm , K^\pm , proton and anti-proton beams", to be published.
8. G. Donaldson et al., "Inclusive η Production at Large Transverse Momenta", to be published.

TABLE I
BEAM FRACTIONS AND CONTAMINATIONS

<u>100 GeV/c</u>			<u>200 GeV/c</u>	
	<u>90°</u>	<u>30° and 10°</u>	<u>90°</u>	<u>30°</u>
<u>Positive Beam</u>			<u>Positive Beam</u>	
p	.222	.229	.684	.7162
K ⁺	.0197	.0166	.0188 (6% π^+)	.0168
π^+	.574	.632	.175	.193
<u>Negative Beam</u>			<u>Negative Beam</u>	
p	.0192	.0185 (9%K ⁻)	.0132 (8% π^-)	.0077 (23% π^- and 6%K ⁻)
K ⁻	.0212	.0196	.0356 (22% π^-)	.0236
π^-	.828	.871	.767	.775

Table I: Beam fractions (ratio of unambiguous Cerenkov signatures/total) for runs triggering only on an incident beam particle. Changes in pressure settings and optical alignments account for the differences between beam composition at "90°" and "30°".

TABLE II

Table II: Values obtained for least squares fit to the form

$$E \frac{d\sigma}{dp}^3 = A \frac{(1-x_D)^F}{(p_{\perp}^2 + m^2)^N}, \text{ where } x_D = (x_{\perp}^2 + [x_W - x_0]^2)^{1/2}$$

(Fits for $x_W < 0.8$).

Beam Particle (Beam momenta fit) GeV	A ($\times 10^{-25} \text{ cm}^2/\text{GeV}^2$)	F	x_0	N	m^2	χ^2/DOF
pp (100,200,300)	0.122 ± 0.015	4.42 ± 0.05	0.02 ± 0.01	4.90 ± 0.06	0.81 ± 0.04	306/142
$\pi^- p$ (100,200)	0.113 ± 0.015	3.13 ± 0.10	0.14 ± 0.01	5.06 ± 0.06	0.97 ± 0.04	271/132
$\pi^+ p$ (100,200)	0.102 ± 0.015	3.29 ± 0.10	0.14 ± 0.01	5.00 ± 0.07	0.95 ± 0.04	325/130

FIGURE CAPTIONS

Fig. 1: Peyrou plots displaying the angular acceptance and regions of data collected in E268. Data was collected at three energies: 100, 200 and 300 GeV/c (top to bottom, respectively). Regions of angular acceptance are cross-hatched to display the "90°", "30°" and "10°" settings, and bins wherein the cross section is computed are shaded.

Fig. 2: Symbols denoting intervals of transverse momentum for use on the following figures.

Figs. 3, 5, 7, 9, 11, 13 & 15: The invariant cross section for π^0 production versus $x_{||}$ for the reaction (and at the beam energy) indicated in the heading. The cross sections are computed in intervals of p_{\perp} and $x_{||}$, with the symbols of Fig. 2 showing which p_{\perp} interval is denoted by a particular symbol. Smooth curves represent the parameterization whose values are given in Table II.

Figs. 4, 6, 8 10, 12, 14 & 16: The invariant cross section versus $\theta_{c.m.}$ for the reaction (and at the beam energy) indicated in the heading. The points plotted at the $\theta_{c.m.}$ corresponding to the bin centers of the p_{\perp} , $x_{||}$ bins of the preceding figure. The smooth curves represent the parameterization given in Table II.

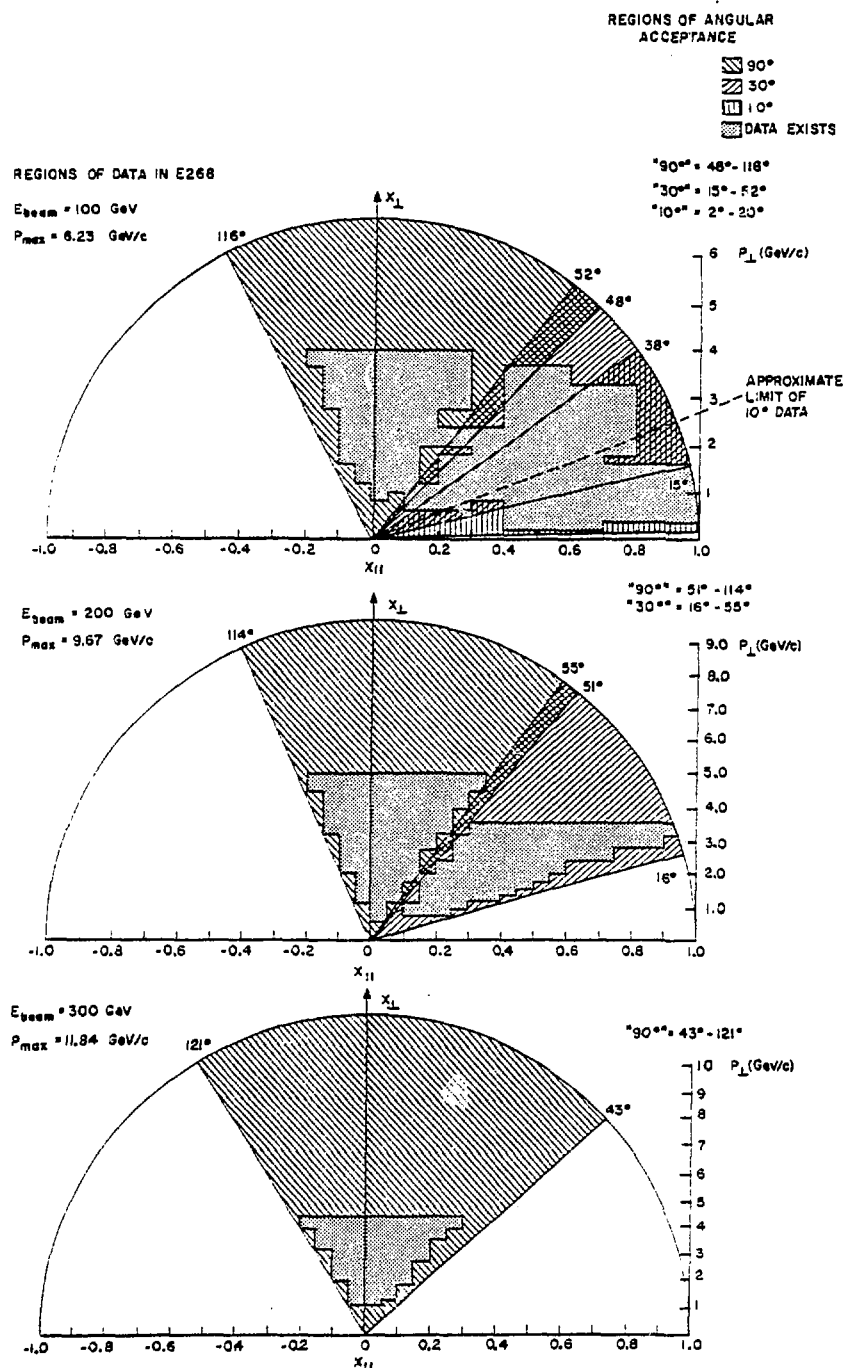


Fig. 1

$E \frac{d\sigma}{dp^3} (\frac{\text{cm}^2}{\text{GeV}^2})$ for Beam + p $\rightarrow \pi^0 + X$ @ 100 GeV/c

p_\perp (GeV/c)	X_{II}	π^+	π^-	p
.2 .4	.40 .50	2.47(.35)E-27	2.06(.29)E-27	1.53(.24)E-27
	.50 .60	1.42(.20)E-27	1.71(.24)E-27	1.02(.14)E-27
	.40 .50	1.01(.14)E-27	1.22(.17)E-27	4.59(.64)E-28
	.50 .60	6.76(.95)E-28	6.10(.85)E-28	3.21(.45)E-28
	.60 .70	3.68(.52)E-28	3.73(.52)E-28	1.58(.26)E-28
	.70 .80	2.39(.34)E-28	2.63(.37)E-28	1.58(.22)E-29
	.80 .90	1.77(.25)E-28	2.00(.28)E-28	3.46(.61)E-30
	.90 1.00	6.94(.97)E-29	9.17(1.28)E-29	
	.15 .25	1.01(.14)E-27	1.20(.17)E-27	1.10(.15)E-27
	.40 .50	5.53(.77)E-28	6.80(.95)E-28	3.00(.42)E-28
.4 .6	.50 .60	3.23(.45)E-28	3.95(.55)E-28	1.07(.17)E-28
	.60 .70	1.95(.27)E-28	2.15(.30)E-28	
	.70 .80	7.42(1.04)E-29	8.71(1.22)E-29	8.70(1.22)E-30
	.80 .90	4.14(.58)E-29	5.00(.70)E-29	2.59(.65)E-30
	.90 1.00	1.11(.16)E-29	1.22(.17)E-29	
	.15 .25	1.01(.14)E-27	1.20(.17)E-27	1.10(.15)E-27
	.40 .50	5.53(.77)E-28	6.80(.95)E-28	3.00(.42)E-28
	.50 .60	3.23(.45)E-28	3.95(.55)E-28	1.07(.17)E-28
	.60 .70	1.95(.27)E-28	2.15(.30)E-28	
	.70 .80	7.42(1.04)E-29	8.71(1.22)E-29	8.70(1.22)E-30
.6 .8	.80 .90	4.14(.58)E-29	5.00(.70)E-29	2.59(.65)E-30
	.90 1.00	1.11(.16)E-29	1.22(.17)E-29	
	.15 .25	1.01(.14)E-27	1.20(.17)E-27	1.10(.15)E-27
	.40 .50	5.53(.77)E-28	6.80(.95)E-28	3.00(.42)E-28
	.50 .60	3.23(.45)E-28	3.95(.55)E-28	1.07(.17)E-28
	.60 .70	1.95(.27)E-28	2.15(.30)E-28	
	.70 .80	7.42(1.04)E-29	8.71(1.22)E-29	8.70(1.22)E-30
	.80 .90	4.14(.58)E-29	5.00(.70)E-29	2.59(.65)E-30
	.90 1.00	1.11(.16)E-29	1.22(.17)E-29	
	.00 .05	2.31(.32)E-28		7.13(1.00)E-28
.8 1.0	.20 .30	3.14(.44)E-28	3.74(.52)E-28	3.13(.44)E-28
	.30 .40	2.75(.39)E-28	4.20(.59)E-28	1.99(.28)E-28
	.40 .50	2.27(.32)E-28	2.30(.32)E-28	8.32(1.47)E-29
	.50 .60	1.44(.20)E-28	1.88(.26)E-28	5.24(.73)E-29
	.60 .70	1.05(.15)E-28	1.15(.16)E-28	
	.70 .80	3.18(.45)E-29	3.75(.53)E-29	3.13(.44)E-30
	.80 .90	1.65(.23)E-29	2.07(.29)E-29	8.27(2.40)E-31
	.90 1.00	2.79(.39)E-30	3.37(.47)E-30	
	.00 .05	9.62(1.35)E-29	1.16(.16)E-28	1.84(.26)E-28
	.05 .10	1.11(.16)E-28	1.28(.18)E-28	1.78(.25)E-28
1.0 1.2	.20 .30	8.58(1.20)E-29	1.10(.15)E-28	8.60(1.20)E-29
	.30 .40	8.86(1.24)E-29	7.43(1.05)E-29	6.46(.90)E-29
	.40 .50	7.34(1.03)E-29	7.94(1.11)E-29	3.00(.62)E-29
	.50 .60	5.87(.82)E-29	5.35(.75)E-29	
	.60 .70	3.18(.45)E-29	3.46(.53)E-29	
	.70 .80	1.20(.17)E-29	1.51(.21)E-29	1.12(.28)E-30
	.80 .90	6.40(.90)E-30	8.44(1.18)E-30	3.09(1.55)E-31
	.90 1.00	6.04(.96)E-31	1.10(.18)E-30	
	-.05 0.00	2.15(.33)E-29	2.59(.36)E-29	4.55(.64)E-29
	0.00 .05	2.84(.40)E-29	3.20(.45)E-29	5.72(.80)E-29
1.2 1.4	.05 .10	4.23(.59)E-29	4.78(.67)E-29	5.33(.75)E-29
	.20 .30	2.37(.33)E-29	3.29(.46)E-29	2.66(.37)E-29

$E \frac{d\sigma}{dp^3} (\frac{\text{cm}^2}{\text{GeV}^2})$ for Beam + p $\rightarrow \pi^0 + X$ @ 100 GeV/c

p_\perp (GeV/c)	X_{II}	π^+	π^-	p
1.2 1.4	.30 .40	2.38(.33)E-29	2.92(.41)E-29	1.74(.24)E-29
	.40 .50	1.94(.27)E-29	2.58(.36)E-29	9.60(1.34)E-30
	.70 .80	4.08(.57)E-30	4.64(.65)E-30	1.83(.92)E-31
	.80 .90	2.11(.30)E-30	2.07(.29)E-30	
	.90 1.00	1.81(.55)E-31	3.74(.94)E-31	
	1.05 0.00	1.01(.30)E-29	6.06(2.00)E-30	1.49(.37)E-29
	0.00 .15	8.26(1.60)E-30	1.12(.16)E-29	1.37(.30)E-29
	.05 .10	1.10(.15)E-29	1.24(.23)E-29	1.81(.25)E-29
	.10 .15	1.33(.24)E-29		1.50(.48)E-29
	.20 .30	1.08(.15)E-29	1.58(.22)E-29	7.92(1.11)E-30
1.4 1.6	.30 .40	8.39(1.18)E-30	1.04(.15)E-29	6.97(2.00)E-30
	.40 .50	5.84(.82)E-30	6.99(.98)E-30	3.27(.46)E-30
	.50 .60	4.86(.68)E-30	3.10(.43)E-30	9.99(4.00)E-31
	.70 .80	1.33(.19)E-30	1.76(.25)E-30	1.12(.68)E-31
	.80 .90	6.31(.88)E-31	6.14(.86)E-31	
	.90 1.00	5.20(3.12)E-32	6.51(3.91)E-32	
	1.05 0.00	4.31(.60)E-30	3.53(.49)E-30	6.82(.96)E-30
	0.00 .05	4.63(.65)E-30	3.59(.50)E-30	6.60(.92)E-30
	.05 .10	4.26(1.20)E-30	3.96(.55)E-30	6.47(.91)E-30
	.10 .15	4.60(2.30)E-30	4.41(.62)E-30	7.74(1.08)E-30
1.6 1.8	.30 .40	3.06(.43)E-30	3.12(.44)E-30	1.88(.26)E-30
	.40 .50	2.08(.29)E-30	2.15(.30)E-30	8.22(1.15)E-31
	.50 .60	1.21(.17)E-30	1.24(.17)E-30	2.43(.34)E-31
	.60 .70	9.21(1.29)E-31	1.15(.16)E-30	1.46(.23)E-31
	1.10 0.00	1.69(.24)E-30	1.62(.44)E-30	2.77(.39)E-30
	0.00 .05	2.06(.29)E-30	1.87(.26)E-30	2.97(.42)E-30
	.05 .10	2.17(.30)E-30	1.63(.23)E-30	2.59(.36)E-30
	.10 .15	2.39(.34)E-30	2.01(.28)E-30	2.81(.39)E-30
	.30 .40	1.33(.19)E-30	1.31(.18)E-30	7.61(1.07)E-31
	.40 .50	9.50(1.33)E-31	9.74(1.36)E-31	3.33(.47)E-31
1.8 2.0	.50 .60	5.43(.76)E-31	5.31(.74)E-31	1.16(.16)E-31
	.60 .70	2.99(.42)E-31	3.36(.47)E-31	2.98(.89)E-32
	.70 .80	1.39(.20)E-31	1.78(.25)E-31	2.38(1.19)E-32
	1.10 0.00	5.21(.73)E-31	4.34(.94)E-31	5.85(.82)E-31
	0.00 .10	5.39(.76)E-31	4.85(.68)E-31	6.15(.86)E-31
	.10 .20	5.92(.83)E-31	6.53(.91)E-31	6.01(.84)E-31
	.30 .40	3.66(.51)E-31	3.94(.55)E-31	2.14(.30)E-31
	.40 .60	2.03(.29)E-31	2.03(.29)E-31	4.59(.64)E-32

$E \frac{d\sigma}{dp^3} (\frac{cm^2}{GeV^2})$ for Beam + p $\rightarrow \pi^0 + X$ @ 100 GeV/c

p_{\perp} (GeV/c)	X_{II}	π^+	π^-	p	
2.0	2.4	.60 .80	5.19(.73)E-32	6.09(.85)E-32	4.92(1.72)E-33
2.4	2.8	-.10 0.00 0.00 .10 .10 .20 .40 .60 .60 .80	7.22(1.01)E-32 9.26(1.30)E-32 9.80(1.37)E-32 3.15(.44)E-32 5.62(.90)F-33	9.33(1.31)E-32 8.91(1.25)E-32 8.21(1.15)E-32 3.76(.53)E-32 1.13(.16)F-32	9.49(1.33)E-32 1.00(.14)E-31 6.74(.94)E-32 6.85(2.06)F-33 4.92(1.72)E-33
2.8	3.2	-.15 .30 .40 .60 .60 .80	1.70(.24)E-32 4.70(.66)E-33 1.46(.51)E-33	1.78(.25)E-32 6.46(1.42)E-33	9.40(1.96)E-33
3.2	3.6	-.15 .30 .40 .60	2.89(.83)E-33 1.34(.67)E-33	5.56(2.00)E-33 2.59(.52)F-33	
3.6	4.0	-.20 .30		9.04(3.98)F-34	

$E \frac{d\sigma}{dp^3} \left(\frac{\text{cm}^2}{\text{GeV}^2} \right)$ for Beam + p $\rightarrow \pi^0 + X$ @ 200 GeV/c

p_T (GeV/c)	X_{II}	π^+	π^-	p
.6 .8	0.00 .05	1.57(.22)E-27	1.40(.20)E-27	1.96(.27)E-27
.8 1.0	0.00 .05	4.87(.68)E-28	4.03(.56)E-28	7.43(1.04)E-28
	.10 .20	4.50(.63)E-28	4.66(.65)E-28	4.88(.68)E-28
1.0 1.2	0.00 .05	1.80(.25)E-28	1.68(.24)E-28	2.15(.30)E-28
	.10 .20	1.70(.24)E-28	1.58(.22)E-28	2.11(.30)E-28
	.20 .30	1.55(.22)E-28	1.61(.23)E-28	1.41(.20)E-28
1.2 1.4	-.05 0.00	3.38(.47)E-29	3.12(.44)E-29	5.40(.76)E-29
	0.00 .05	3.68(.52)E-29	3.39(.47)E-29	5.25(.74)E-29
	.05 .10	5.04(.71)E-29	4.77(.67)E-29	5.60(.78)E-29
	.15 .20	4.02(.56)E-29	6.65(.93)E-29	
	.20 .30	4.67(.66)E-29	4.60(.65)E-29	4.06(.57)E-29
	.30 .40	3.99(.56)E-29	4.28(.60)E-29	2.43(.34)E-29
1.4 1.6	-.05 0.00	1.92(.27)E-29	1.63(.23)E-29	2.59(.36)E-29
	0.00 .05	2.11(.30)E-29	1.77(.25)E-29	2.55(.36)E-29
	.05 .10	2.12(.30)E-29	2.27(.32)E-29	2.70(.38)E-29
	.15 .20	1.65(.23)E-29	2.51(.35)E-29	
	.20 .30	1.69(.24)E-29	1.83(.26)E-29	1.60(.22)E-29
	.30 .40	1.41(.20)E-29	1.84(.26)E-29	8.36(1.17)E-30
	.40 .45	1.31(.18)E-29	1.48(.30)E-29	
1.6 1.8	-.05 0.00	5.63(.79)E-30	6.55(.92)E-30	9.18(1.29)E-30
	0.00 .05	8.13(1.14)E-30	8.35(1.17)E-30	1.02(.14)E-29
	.05 .10	7.55(1.06)E-30	8.73(1.22)E-30	1.03(.14)E-29
	.20 .30	7.39(1.03)E-30	8.65(1.21)E-30	6.07(.85)E-30
	.30 .40	6.32(.89)E-30	5.41(.76)E-30	3.22(.45)E-30
	.40 .50	3.98(.80)E-30	3.95(.55)E-30	1.17(.17)E-30
1.8 2.0	-.05 0.00	2.50(.63)E-30	3.14(.44)E-30	5.05(.71)E-30
	0.00 .10	3.81(.53)E-30	2.96(.41)E-30	4.54(.64)E-30
	.10 .15		2.59(.36)E-30	3.12(.44)E-30
	.20 .30	2.44(.34)E-30	2.16(.30)E-30	1.91(.27)E-30
	.30 .40	1.62(.23)E-30	1.44(.20)E-30	8.80(1.23)E-31
	.40 .50	1.20(.17)E-30	1.15(.16)E-30	4.31(.60)E-31
2.0 2.4	-.10 0.00	7.05(.99)E-31	6.39(.89)E-31	9.26(1.30)E-31
	0.00 .10	6.43(.90)E-31	6.77(.95)E-31	8.25(1.16)E-31
	.10 .15	1.11(.34)E-30		9.30(2.79)E-31
	.20 .30	7.63(1.07)E-31	7.39(1.03)E-31	6.01(.84)E-31
	.30 .40	5.68(.80)E-31	5.35(.75)E-31	3.04(.43)E-31
	.40 .50	3.38(.47)E-31	3.56(.50)E-31	1.30(.18)E-31
	.50 .60	2.45(.34)E-31	2.59(.36)E-31	4.61(.65)E-32

$E \frac{d\sigma}{dp^3} \left(\frac{\text{cm}^2}{\text{GeV}^2} \right)$ for Beam + p $\rightarrow \pi^0 + X$ @ 200 GeV/c

p_\perp (GeV/c)	X_{II}	π^+	π^-	p
2.4 2.8	.10 0.00	1.93(.58)E-31	1.73(.24)E-31	2.25(.32)E-31
	0.00 .10	1.73(.24)E-31	1.85(.26)E-31	2.00(.28)E-31
	.10 .15	1.86(.26)E-31	2.46(.34)E-31	1.89(.26)E-31
	.30 .40	1.14(.16)E-31	1.11(.16)E-31	5.47(.77)E-32
	.40 .50	9.01(1.26)E-32	7.69(1.08)E-32	2.66(.37)E-32
	.50 .60	4.83(.68)E-32	5.44(.76)E-32	8.96(1.37)E-33
	.60 .70			
2.8 3.2	-.10 0.00	4.03(.61)E-32	3.71(.52)E-32	4.02(.56)E-32
	0.00 .10	3.66(.51)E-32	4.26(.60)E-32	4.57(.64)E-32
	.10 .20	5.38(.75)E-32	4.26(1.28)E-32	4.01(.56)E-32
	.30 .40	2.35(.33)E-32	2.55(.36)E-32	1.02(.14)E-32
	.40 .50	1.88(.26)E-32	1.82(.26)E-32	5.06(1.01)E-33
	.50 .60	1.00(.20)E-32	1.31(.18)E-32	1.38(.28)E-33
	.60 .70		6.83(.96)E-33	1.08(.44)E-33
3.2 3.6	-.15 0.00	1.10(.50)E-32	9.23(2.01)E-33	7.53(1.05)E-33
	0.00 .10	8.87(1.80)E-33	1.18(.17)E-32	8.72(2.62)E-33
	.10 .20	6.67(2.00)E-33	9.80(1.37)E-33	7.29(1.46)E-33
	.30 .50	6.83(1.57)E-33	4.36(.61)E-33	1.66(.37)E-33
	.50 .70	2.46(.86)E-33	1.78(.25)E-33	4.70(2.35)E-34
	-.15 .25	1.34(.67)E-33	2.27(.32)E-33	1.37(.34)E-33
	.35 .55	9.85(5.91)E-34	1.21(.43)E-33	3.38(2.03)E-34
4.0 4.5	.55 .75		2.15(1.72)E-34	
	-.15 .30		6.08(1.82)E-34	4.39(1.10)E-34
	.35 .55		2.15(2.16)E-34	
4.5 5.0	-.20 .35		2.69(1.35)E-34	

$E \frac{d\sigma}{dp_3} \left(\frac{\text{cm}^2}{\text{GeV}^2} \right)$ for Beam + p $\rightarrow \pi^0 + X$ @ 300 GeV/c

p_\perp (GeV/c)	$X_{ }$	π^+	π^-	p
1.2 1.4	-.05 0.00			5.84 (.82) E-29
	0.00 .05			6.61 (.93) E-29
	.05 .10			5.96 (.83) E-29
1.4 1.6	-.05 0.00			1.97 (.28) E-29
	0.00 .05			2.67 (.37) F-29
	.05 .10			2.43 (.34) E-29
1.6 1.8	-.05 0.00			7.19 (1.01) E-30
	0.00 .05			1.11 (.16) E-29
	.05 .10			1.17 (.16) E-29
1.8 2.0	-.05 0.00			4.72 (.66) E-30
	0.00 .05			3.97 (.56) E-30
	.05 .10			3.67 (.51) E-30
	.10 .15			3.72 (.93) E-30
2.0 2.4	-.10 0.00			1.04 (.15) E-30
	0.00 .10			8.70 (1.22) E-31
	.10 .15			9.94 (1.39) E-31
2.4 2.8	-.10 0.00			1.97 (.28) E-31
	0.00 .10			2.27 (.32) E-31
2.8 3.2	-.10 0.00			5.47 (.77) E-32
	0.00 .10			4.67 (.66) E-32
	.10 .20			3.08 (.43) E-32
3.2 3.6	-.10 0.00			1.32 (.28) E-32
	0.00 .10			1.63 (.23) E-32
	.10 .20			1.14 (.16) E-32
3.6 4.0	-.10 0.00			5.52 (2.05) E-33
	0.00 .10			5.03 (1.18) E-33
4.0 4.5	-.10 .30			7.93 (2.86) E-34

$E \frac{d\sigma}{dp^3} \left(\frac{\text{cm}^2}{\text{GeV}^2} \right)$ for Beam + p $\rightarrow \pi^0 + X$ @ 100 GeV/c

p_t (GeV/c)	X_{II}	p	K^+	π^+	\bar{p}	K^-	π^-
.4	.6	.70 .95	$9.40(1.32)\epsilon^{-30}$	$7.09(1.99)\epsilon^{-29}$	$1.83(1.26)\epsilon^{-28}$	$2.99(1.42)\epsilon^{-27}$	$1.20(1.17)\epsilon^{-27}$
.6	.8	.15 .25	$1.10(1.15)\epsilon^{-27}$	$6.86(2.13)\epsilon^{-28}$	$1.01(1.14)\epsilon^{-27}$	$6.18(2.62)\epsilon^{-30}$	$3.98(1.60)\epsilon^{-29}$
.8	1.0	0.00 .05	$4.84(1.68)\epsilon^{-30}$	$2.80(1.42)\epsilon^{-29}$	$4.91(1.69)\epsilon^{-29}$	$6.18(1.62)\epsilon^{-30}$	$5.79(1.61)\epsilon^{-29}$
1.0	1.2	0.00 .10	$7.13(1.00)\epsilon^{-28}$	$2.95(1.48)\epsilon^{-28}$	$2.76(1.41)\epsilon^{-28}$	$4.48(1.12)\epsilon^{-28}$	$4.12(1.58)\epsilon^{-28}$
1.2	1.5	.40	$2.82(1.40)\epsilon^{-28}$	$2.07(1.41)\epsilon^{-28}$	$3.02(1.42)\epsilon^{-28}$	$6.25(1.88)\epsilon^{-26}$	$4.12(1.12)\epsilon^{-26}$
1.5	.70 .95	$1.83(1.26)\epsilon^{-30}$	$5.84(1.75)\epsilon^{-30}$	$2.01(1.28)\epsilon^{-29}$	$5.02(1.86)\epsilon^{-30}$	$1.20(1.26)\epsilon^{-29}$	$2.41(1.34)\epsilon^{-29}$
2.0	.20 .55	$1.54(1.22)\epsilon^{-29}$	$8.83(2.21)\epsilon^{-29}$	$1.04(1.15)\epsilon^{-28}$	$1.97(1.43)\epsilon^{-28}$	$8.07(3.23)\epsilon^{-29}$	$1.20(1.17)\epsilon^{-28}$
2.5	.70 .95	$6.37(1.34)\epsilon^{-31}$	$1.12(1.45)\epsilon^{-30}$	$7.51(1.05)\epsilon^{-30}$	$1.39(1.84)\epsilon^{-30}$	$3.91(1.17)\epsilon^{-30}$	$9.37(1.31)\epsilon^{-29}$
3.0	1.2	1.4 -.05	$5.39(1.76)\epsilon^{-29}$	$2.00(1.80)\epsilon^{-29}$	$3.18(1.45)\epsilon^{-29}$	$4.59(2.07)\epsilon^{-29}$	$3.72(1.52)\epsilon^{-29}$
3.5	.20	.55	$1.54(1.22)\epsilon^{-29}$	$1.11(1.16)\epsilon^{-29}$	$2.24(1.31)\epsilon^{-29}$	$1.75(1.61)\epsilon^{-29}$	$1.64(1.58)\epsilon^{-29}$
4.0	.70	.95	$7.86(3.93)\epsilon^{-32}$	$1.03(1.52)\epsilon^{-30}$	$2.56(1.36)\epsilon^{-30}$	$1.78(1.80)\epsilon^{-30}$	$2.83(1.40)\epsilon^{-30}$
4.4	1.6	-.05 .15	$1.50(1.21)\epsilon^{-29}$	$7.07(3.54)\epsilon^{-30}$	$1.06(1.15)\epsilon^{-29}$	$1.08(1.65)\epsilon^{-29}$	$1.20(1.17)\epsilon^{-29}$
5.0	.20	.65	$4.31(1.60)\epsilon^{-30}$	$7.05(1.99)\epsilon^{-30}$	$1.21(1.42)\epsilon^{-29}$	$9.10(1.27)\epsilon^{-30}$	
5.5	.70	.95	$6.67(1.93)\epsilon^{-30}$	$3.73(1.52)\epsilon^{-30}$	$4.68(1.66)\epsilon^{-30}$	$5.52(1.11)\epsilon^{-30}$	$6.25(4.38)\epsilon^{-31}$
6.0	1.6	-.10 .15	$9.54(1.34)\epsilon^{-31}$	$1.08(1.15)\epsilon^{-30}$	$1.95(1.27)\epsilon^{-30}$	$1.30(1.18)\epsilon^{-30}$	$2.41(1.72)\epsilon^{-30}$
6.5	.25	.75	$2.08(1.39)\epsilon^{-30}$	$1.50(1.21)\epsilon^{-30}$	$1.96(1.28)\epsilon^{-30}$	$1.11(1.28)\epsilon^{-30}$	$3.75(1.53)\epsilon^{-30}$
7.0	2.0	-.10 .15	$3.17(1.44)\epsilon^{-31}$	$4.55(1.64)\epsilon^{-31}$	$6.73(1.94)\epsilon^{-31}$	$2.82(1.42)\epsilon^{-31}$	$1.31(1.18)\epsilon^{-30}$
7.5	.25	.85	$7.37(1.12)\epsilon^{-31}$	$4.67(1.65)\epsilon^{-31}$	$6.11(1.86)\epsilon^{-31}$	$4.63(1.74)\epsilon^{-31}$	$4.22(1.59)\epsilon^{-31}$
8.0	2.4	-.10 .20	$4.88(1.68)\epsilon^{-32}$	$6.22(2.49)\epsilon^{-32}$	$1.35(1.19)\epsilon^{-31}$	$3.78(1.14)\epsilon^{-32}$	$6.87(1.24)\epsilon^{-31}$
8.5	.30	.95	$7.09(1.99)\epsilon^{-32}$	$5.66(2.27)\epsilon^{-32}$	$8.82(1.24)\epsilon^{-32}$	$1.12(1.22)\epsilon^{-31}$	$8.93(1.34)\epsilon^{-32}$
9.0	2.8	3.2	$3.92(1.78)\epsilon^{-33}$	$1.40(1.70)\epsilon^{-32}$	$1.57(1.22)\epsilon^{-32}$	$4.16(1.67)\epsilon^{-32}$	$3.77(1.13)\epsilon^{-32}$
9.5	3.2	3.6	$1.58(1.29)\epsilon^{-32}$	$2.23(1.12)\epsilon^{-32}$	$1.56(1.22)\epsilon^{-32}$	$2.89(1.63)\epsilon^{-33}$	$1.94(1.27)\epsilon^{-32}$
10.0	3.6	4.0	$1.34(1.67)\epsilon^{-33}$	$1.40(1.60)\epsilon^{-33}$	$1.34(1.60)\epsilon^{-33}$	$5.56(2.00)\epsilon^{-33}$	

$E \frac{d\sigma}{dp^3} (\frac{\text{cm}^2}{\text{GeV}^2})$ for Beam + p $\rightarrow \pi^0 + X$ @ 200 GeV/c

p_t (GeV/c)	X_{II}	p	K ⁺	π^+	\bar{p}	K ⁻	π^-
.6 .8	0.00 .05	1.96(.27)E-27		1.57(.22)E-27		8.11(1.30)E-28	1.40(.20)E-27
.8 1.0	0.00 .05	7.43(1.04)E-28	4.58(1.37)E-28	4.87(.68)E-28		4.76(.72)E-28	4.03(.56)E-28
	.10 .25	4.53(.64)E-28	2.36(.59)E-28	4.46(.62)E-28	7.20(1.07)E-28	3.83(.54)E-28	4.69(.66)E-28
1.0 1.2	0.00 .05	2.15(.30)E-28		1.80(.25)E-28		1.56(.39)E-28	1.68(.24)E-28
	.10 .30	1.75(.25)E-28	6.80(2.72)E-29	1.58(.22)E-28	2.53(.51)E-28	1.18(.17)E-28	1.55(.22)E-28
1.2 1.4	-.05 .10	5.76(.81)E-29	5.06(.71)E-29	5.29(.74)E-29		3.42(.48)E-29	3.60(.51)E-29
	.15 .40	3.63(.51)E-29	2.66(.37)E-29	4.74(.66)E-29	4.19(.59)E-29	4.11(.58)E-29	4.48(.63)E-29
1.4 1.6	-.05 .10	2.56(.36)E-29	1.79(.25)E-29	1.93(.27)E-29		1.34(.19)E-29	1.87(.26)E-29
	.15 .45	1.24(.17)E-29	1.01(.21)E-29	1.63(.23)E-29	1.68(.25)E-29	1.61(.23)E-29	1.92(.27)E-29
1.6 1.8	-.05 .10	9.86(1.38)E-30	8.15(1.14)E-30	7.49(1.05)E-30		5.84(.82)E-30	7.92(1.11)E-30
	.15 .50	4.43(.62)E-30	8.78(2.20)E-30	6.47(.91)E-30	5.60(1.23)E-30	4.34(.70)E-30	6.89(.96)E-30
1.8 2.0	-.05 .15	4.33(.61)E-30	2.85(.57)E-30	3.77(.59)E-30	3.74(1.68)E-30	1.47(.44)E-30	2.90(.41)E-30
	.15 .55	1.30(.18)E-30	1.32(.19)E-30	1.76(.25)E-30	1.74(.24)E-30	1.29(.18)E-30	1.64(.23)E-30
2.0 2.4	-.10 .15	1.02(.14)E-30	9.59(1.34)E-31	9.70(1.36)E-31	5.59(.78)E-31	4.29(.60)E-31	8.23(1.15)E-31
	.20 .60	2.66(.37)E-31	3.00(.42)E-31	4.75(.67)E-31	3.14(.44)E-31	3.94(.55)E-31	4.69(.66)E-31
2.4 2.8	-.10 .15	1.85(.26)E-31	1.38(.25)E-31	1.84(.26)E-31	1.51(.21)E-31	1.08(.15)E-31	1.90(.27)E-31
	.25 .75	2.85(.40)E-32	4.04(.57)E-32	7.27(1.02)E-32		5.48(.77)E-32	6.70(.94)E-32
2.8 3.2	-.10 .20	4.20(.59)E-32	6.53(1.44)E-32	4.63(.65)E-32	4.23(1.27)E-32	3.87(.58)E-32	4.16(.58)E-32
	.25 .90	4.12(.58)E-33	1.09(.33)E-32	9.62(1.35)E-33		4.67(1.87)E-33	1.27(.18)E-32
3.2 3.6	-.15 .25	5.81(.87)E-33		1.03(.21)E-32		9.00(1.80)E-33	1.11(.16)E-32
	.30 .95	7.01(1.05)E-34		2.78(.42)E-33			
3.6 4.0	-.15 .25	1.37(.34)E-33		1.34(.67)E-33			2.27(.34)E-33
4.0 4.5	-.15 .30	4.39(1.10)E-34					6.08(1.82)E-34
4.5 5.0	-.20 .35						2.69(1.35)E-34

- . 2 < P_{\perp} < . 4
- . 4 < P_{\perp} < . 6
- △ . 6 < P_{\perp} < . 8
- + . 8 < P_{\perp} < 1. 0
- × 1. 0 < P_{\perp} < 1. 2
- ◊ 1. 2 < P_{\perp} < 1. 4
- ▽ 1. 4 < P_{\perp} < 1. 6
- 1. 6 < P_{\perp} < 1. 8
- * 1. 8 < P_{\perp} < 2. 0
- ♦ 2. 0 < P_{\perp} < 2. 4
- ⊕ 2. 4 < P_{\perp} < 2. 8
- 2. 8 < P_{\perp} < 3. 2
- 3. 2 < P_{\perp} < 3. 6
- 3. 6 < P_{\perp} < 4. 0
- 4. 0 < P_{\perp} < 4. 5
- 4. 5 < P_{\perp} < 5. 0
- 5. 0 < P_{\perp} < 5. 5
- △ 6. 0 < P_{\perp} < 6. 5

Symbols Denoting Intervals of Transverse Momentum

$\pi^+ p \rightarrow \pi^0 + X$ @ 100 GeV/c

BNL/CIT/LBL

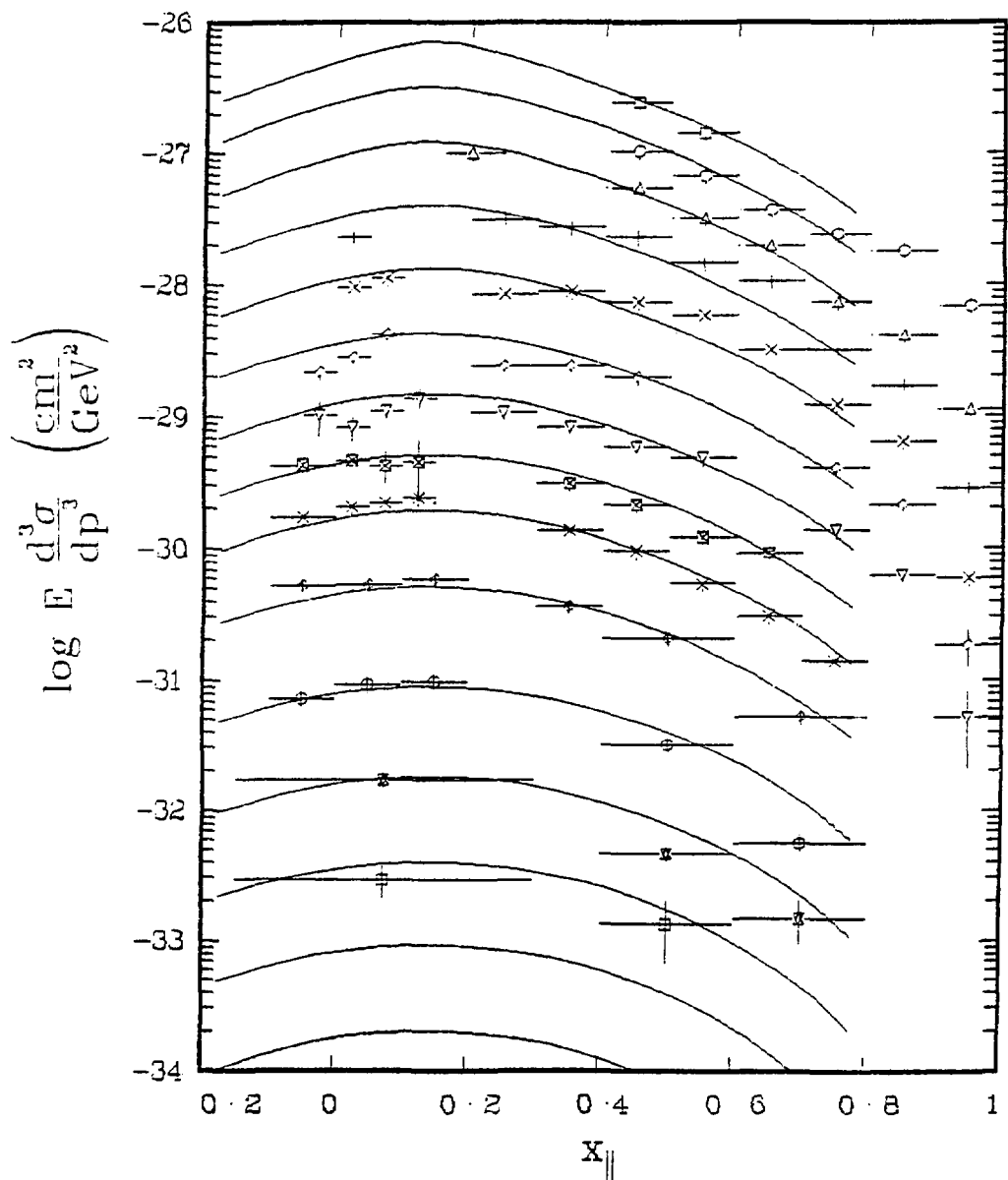


Fig. 3

$\pi^- p \rightarrow \pi^+ + X$ @ 100 GeV/c

BNL/CIT/LBL

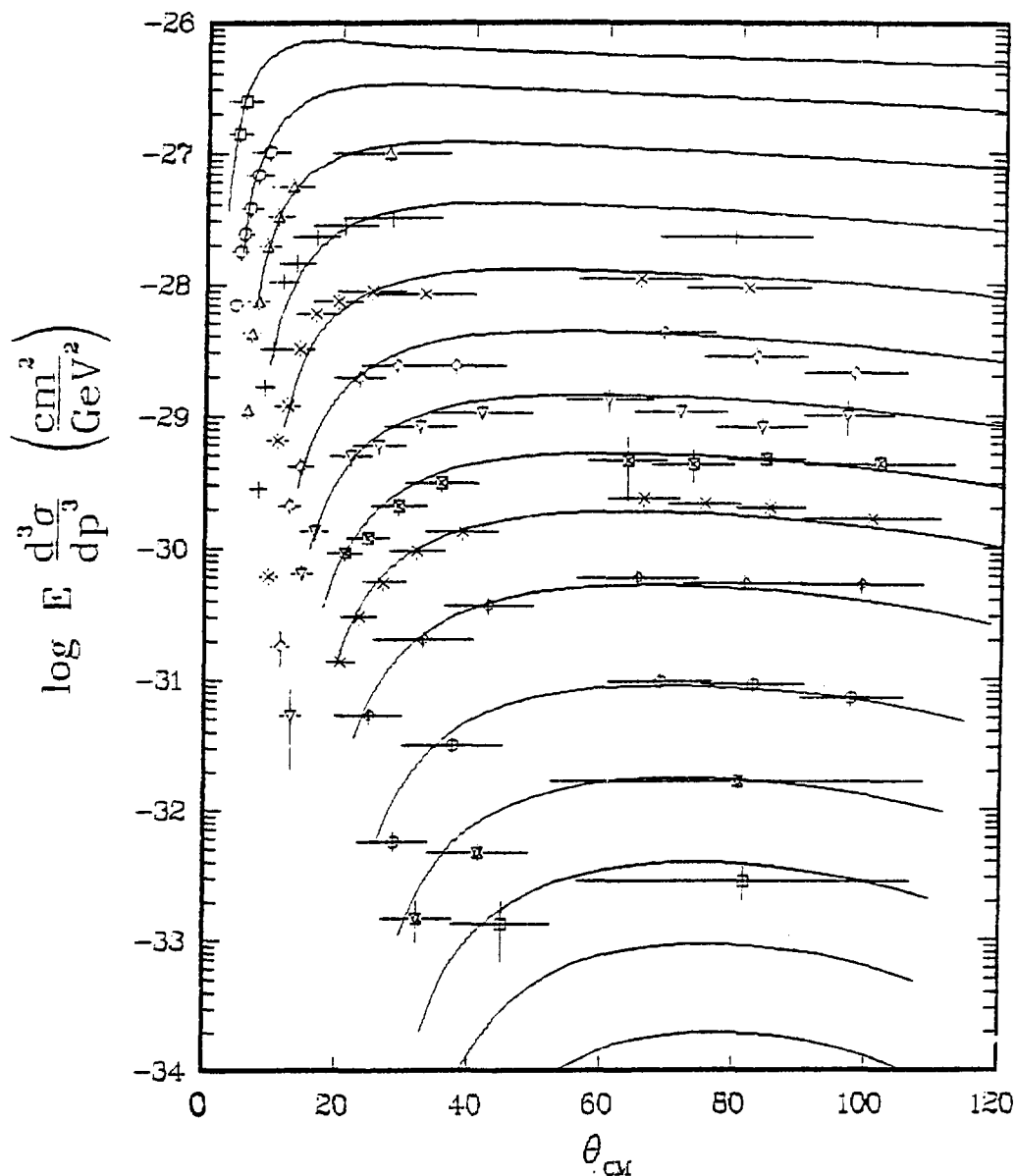


Fig. 4

$\pi^- p \rightarrow \pi^+ + X$ @ 100 GeV/c

BNL/CIT/LBL

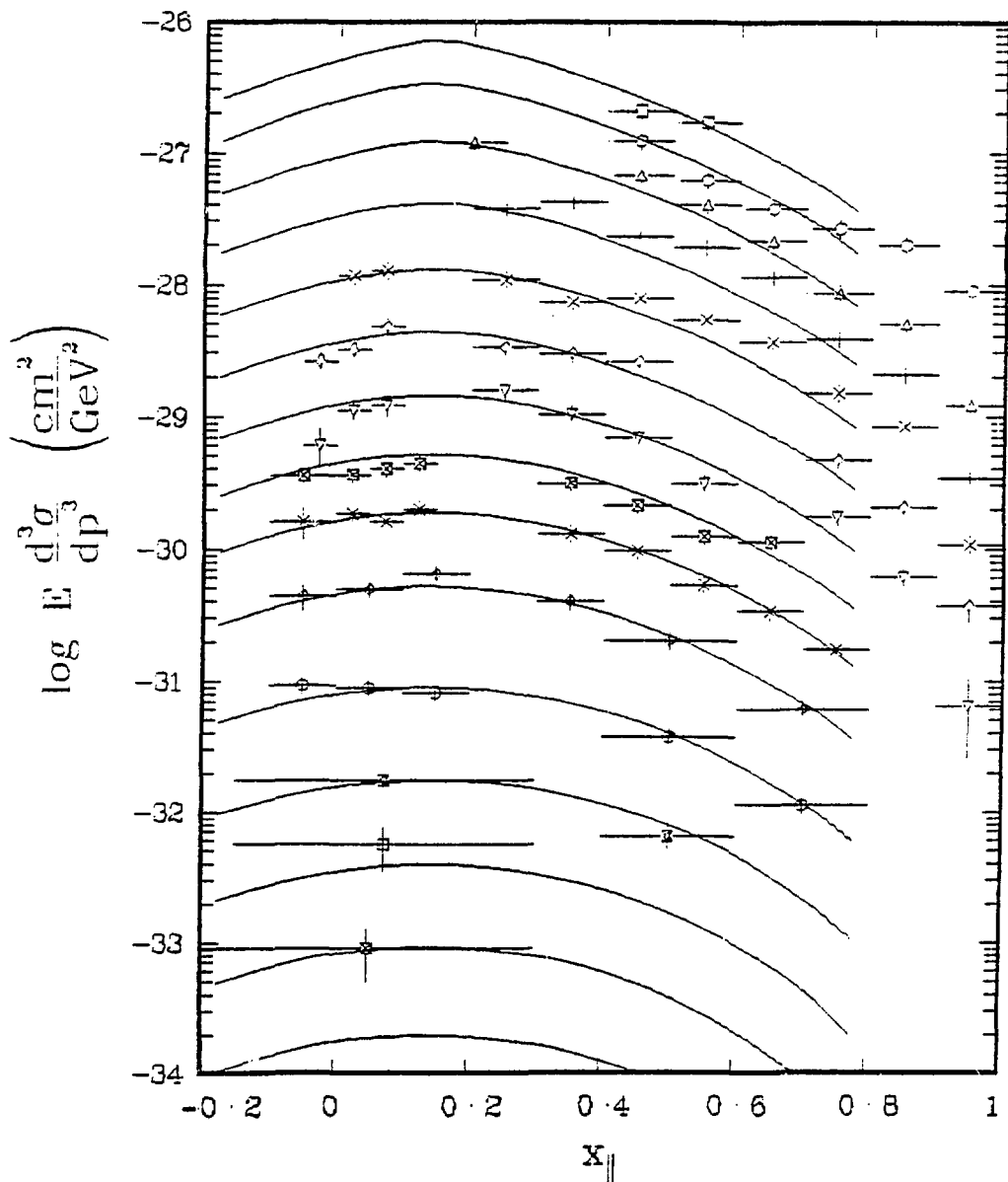


Fig. 5

$\pi^- p \rightarrow \pi^0 + X$ @ 100 GeV/c

BNL/CIT/LBL

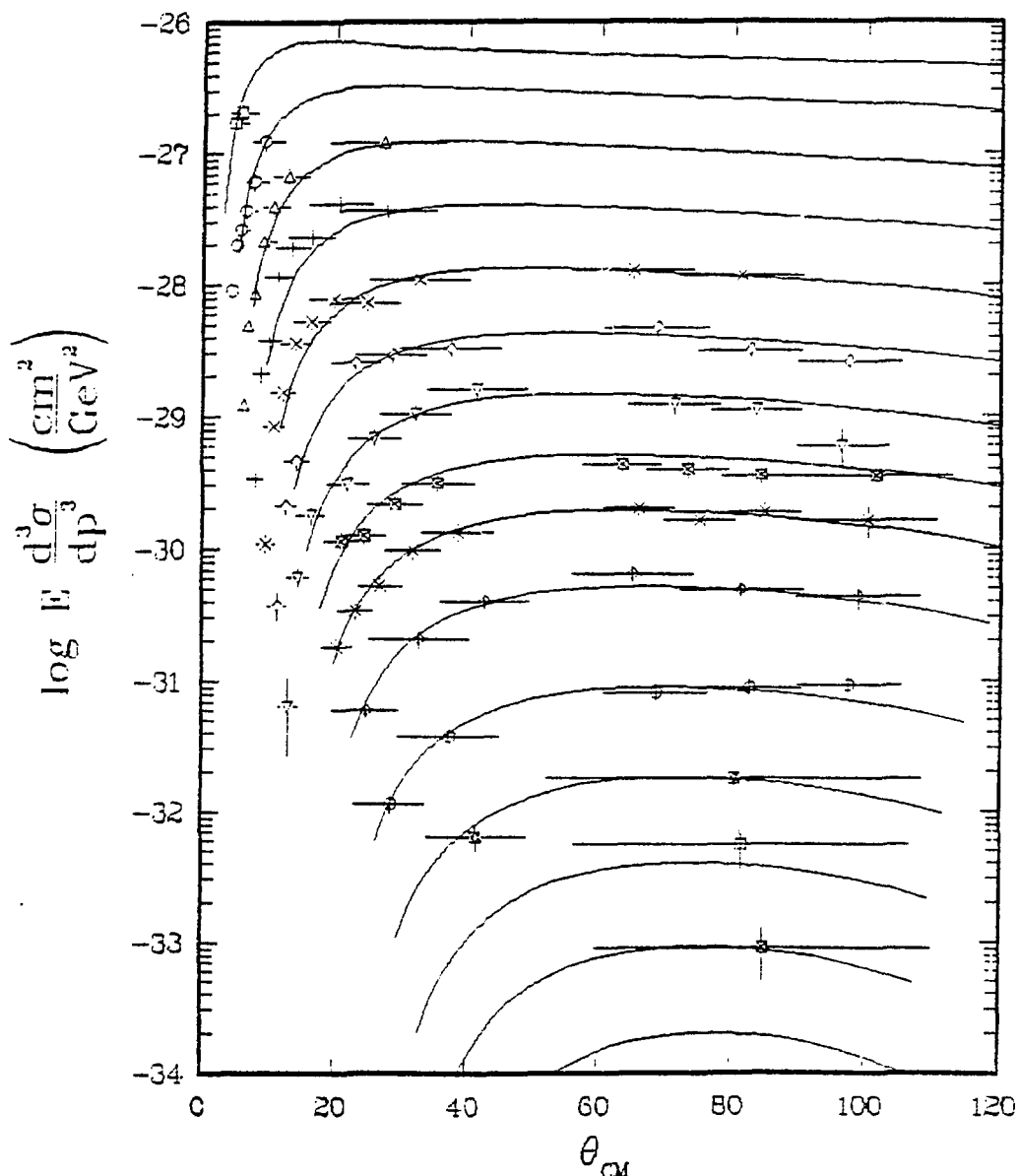


Fig. 6

pp $\rightarrow\pi^0+X$ @ 100 GeV/c

BNL/CIT/LBL

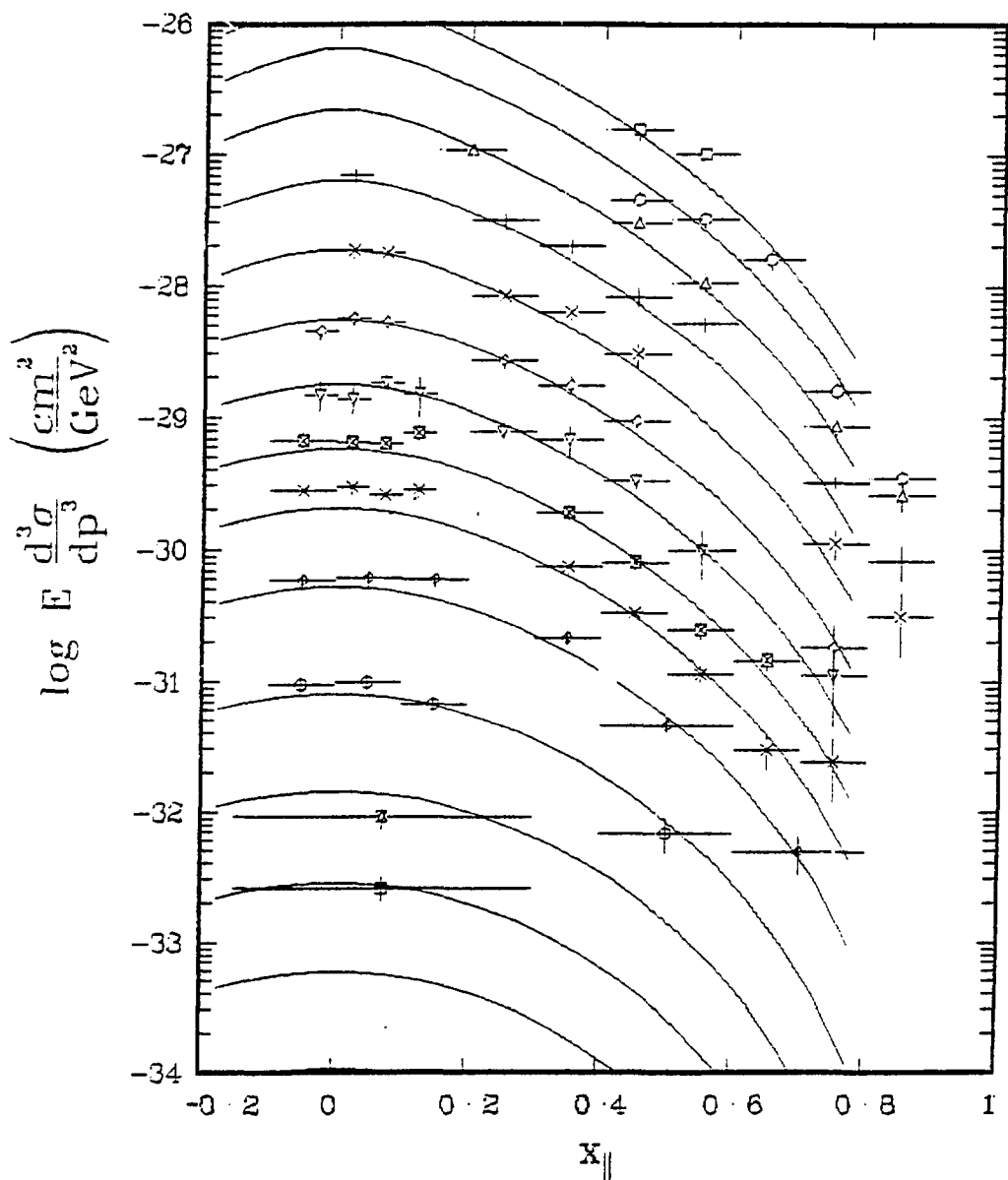


Fig. 7

pp $\rightarrow\pi^{\nu}+X$ @ 100 GeV/c

BNL/CIT/LBL

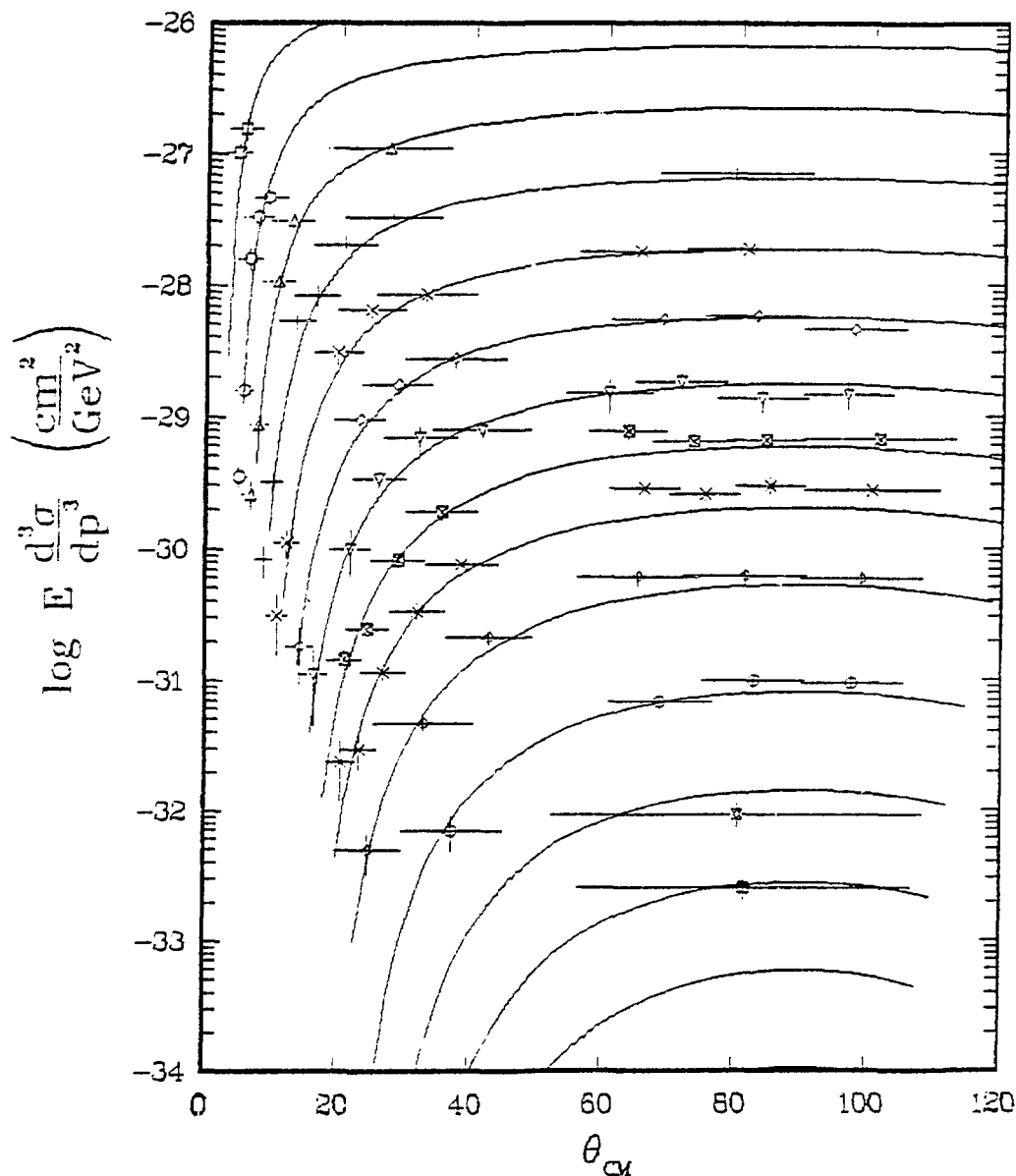


Fig. 8

$\pi^+ p \rightarrow \pi^0 + X$ @ 200 GeV/c

BNL/CIT/LBL

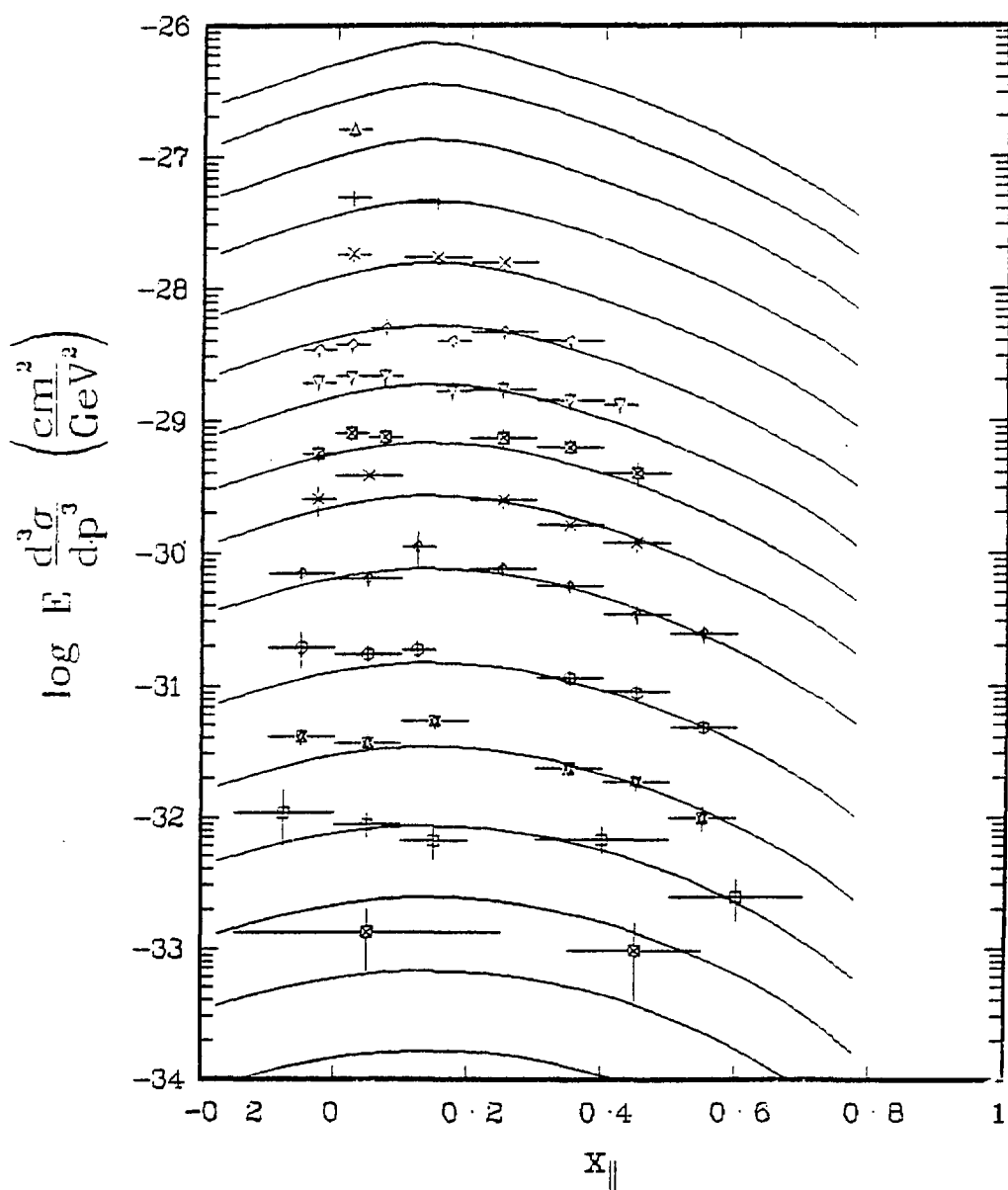


Fig. 9

$\pi^- p \rightarrow \pi^0 + X$ @ 200 GeV/c

BNL/CIT/LBL

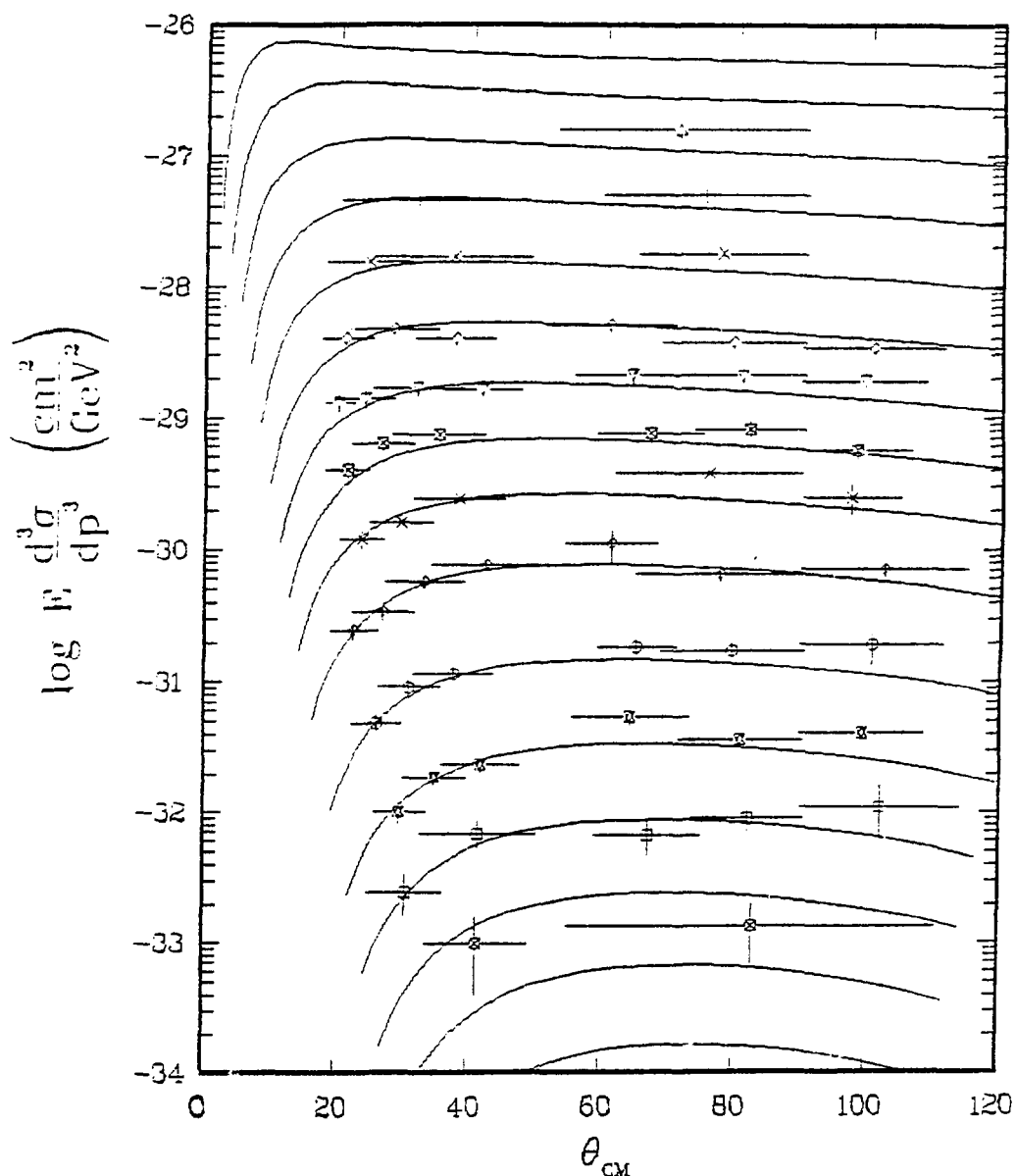


Fig. 10

$\pi^- p \rightarrow \pi^0 + X$ @ 200 GeV/c

BNL/CIT/LBL

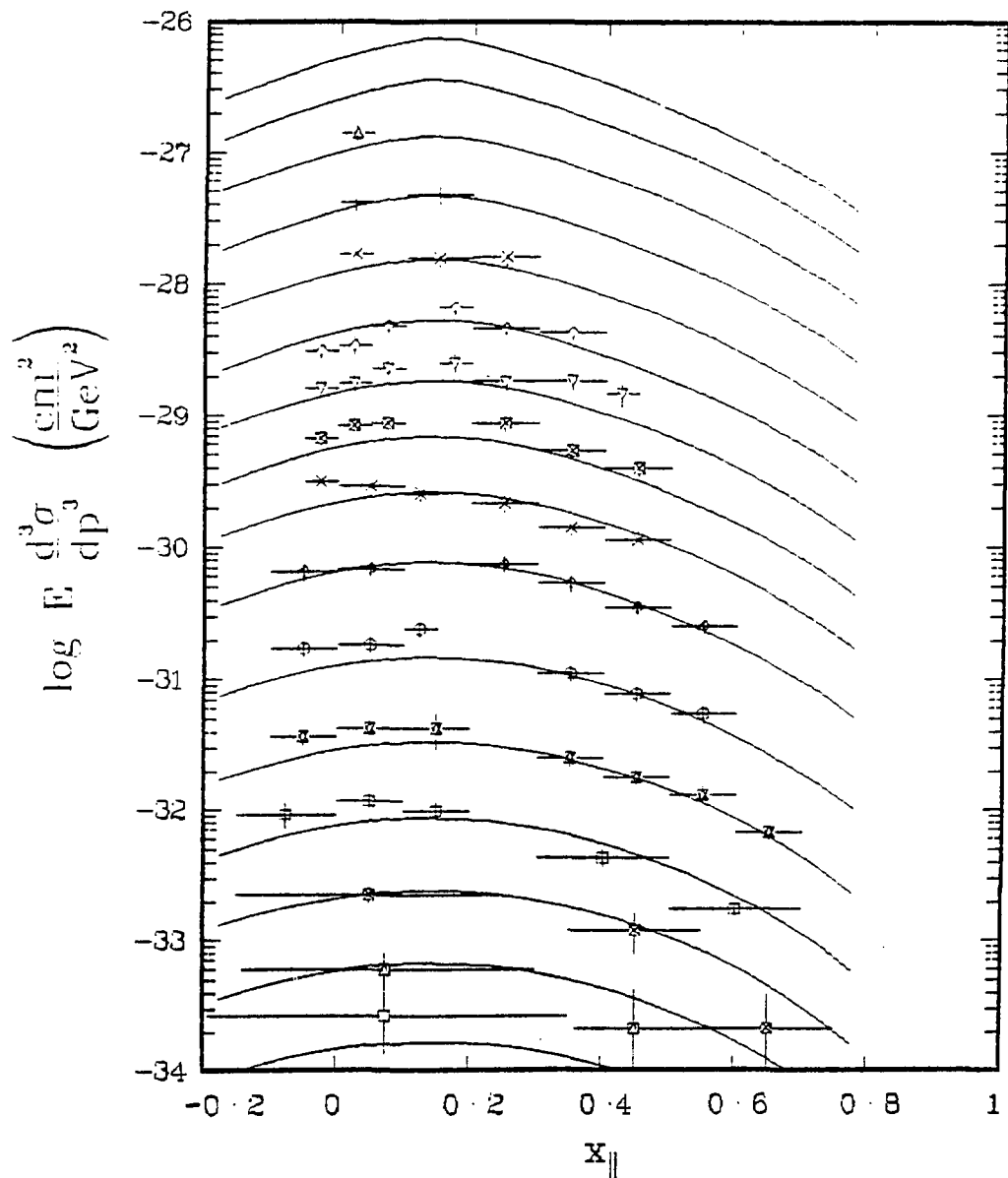


Fig. 11

$\pi^- p \rightarrow \pi^0 + X$ @ 200 GeV/c

BNL/CIT/LBL

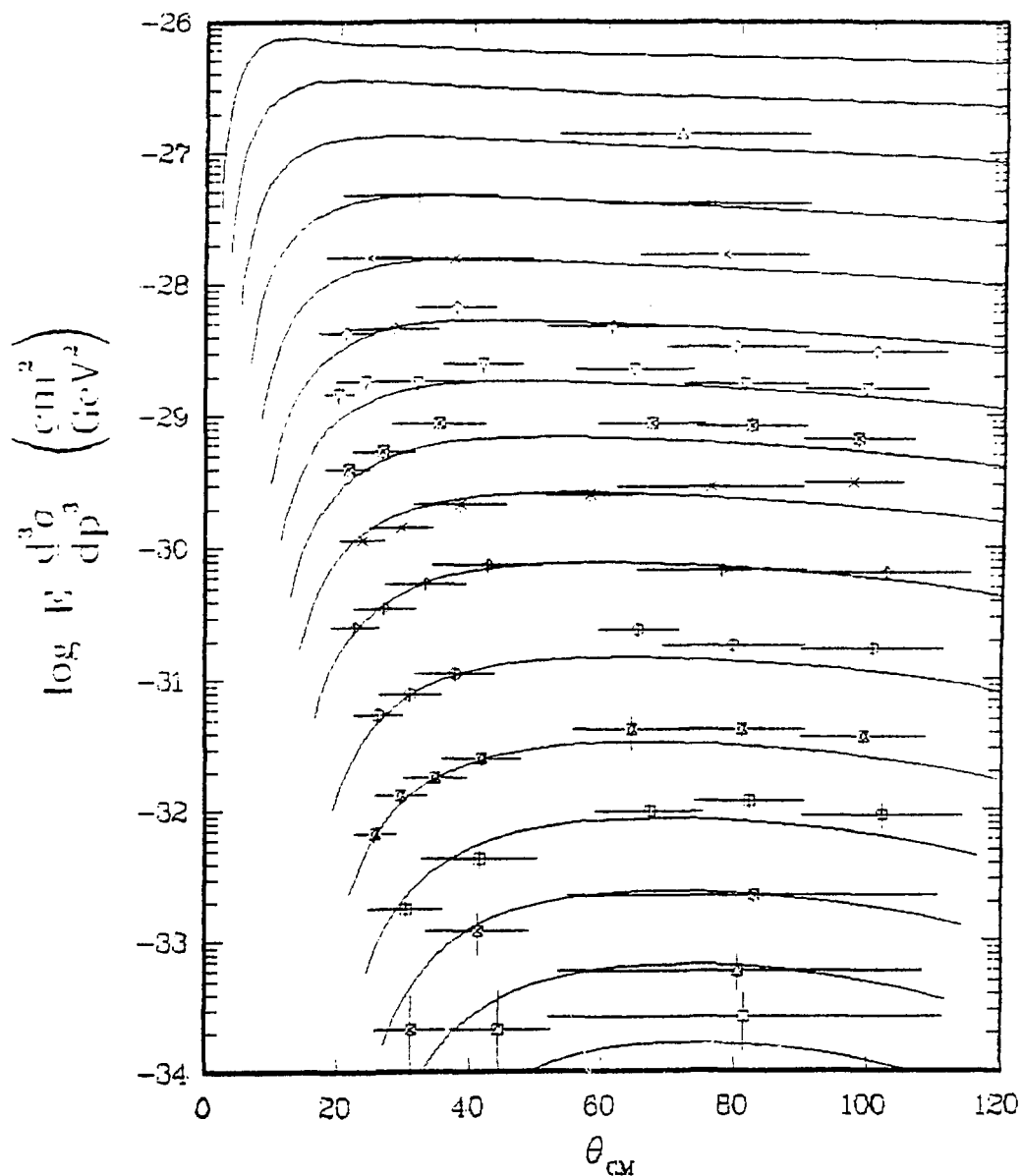


Fig. 12

pp $\rightarrow\pi^{\nu}+X$ @ 200 GeV/c
BNL/CIT/LBL

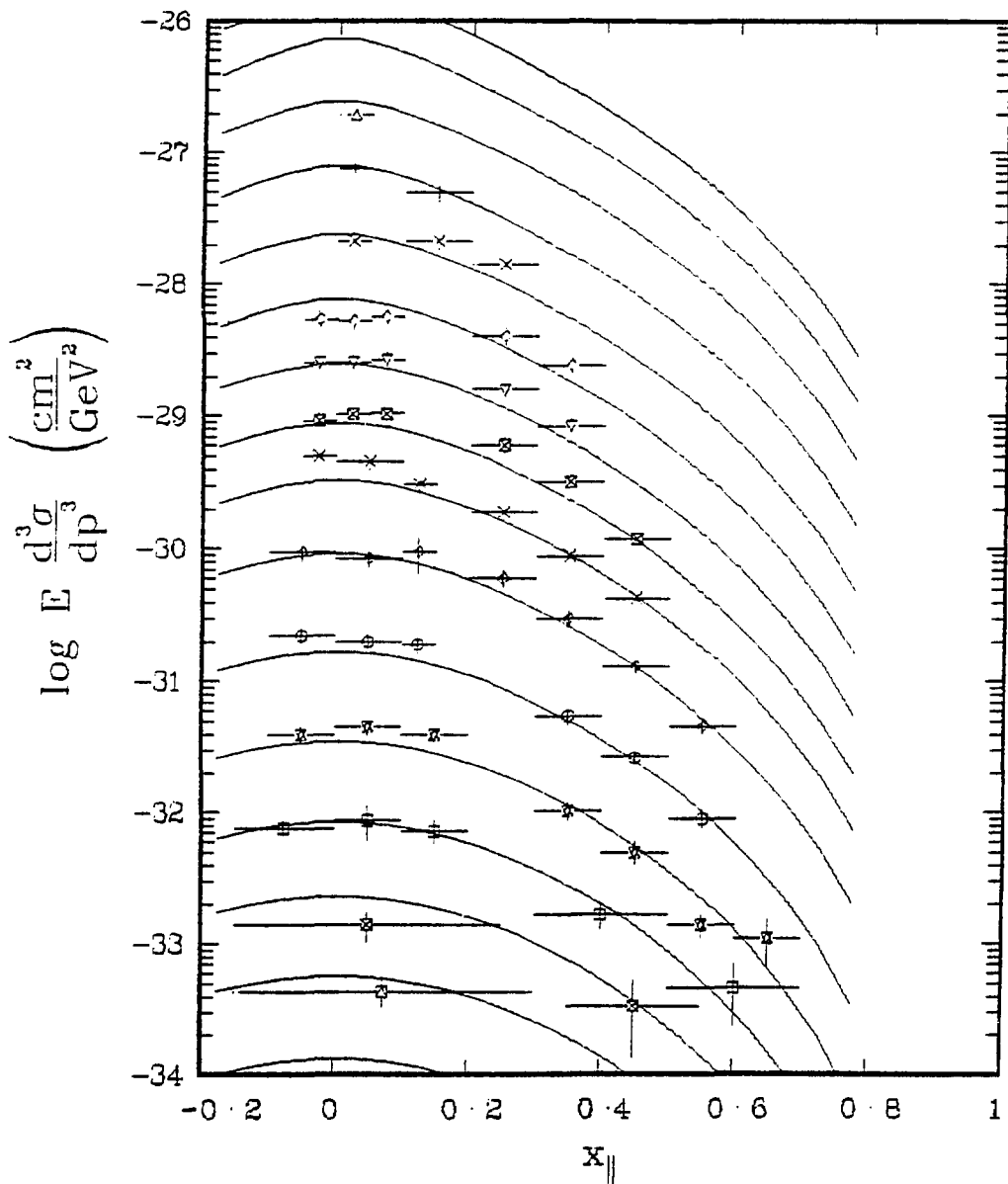


Fig. 13

pp $\rightarrow\pi^0+X$ @ 200 GeV/c

BNL/CIT/LBL

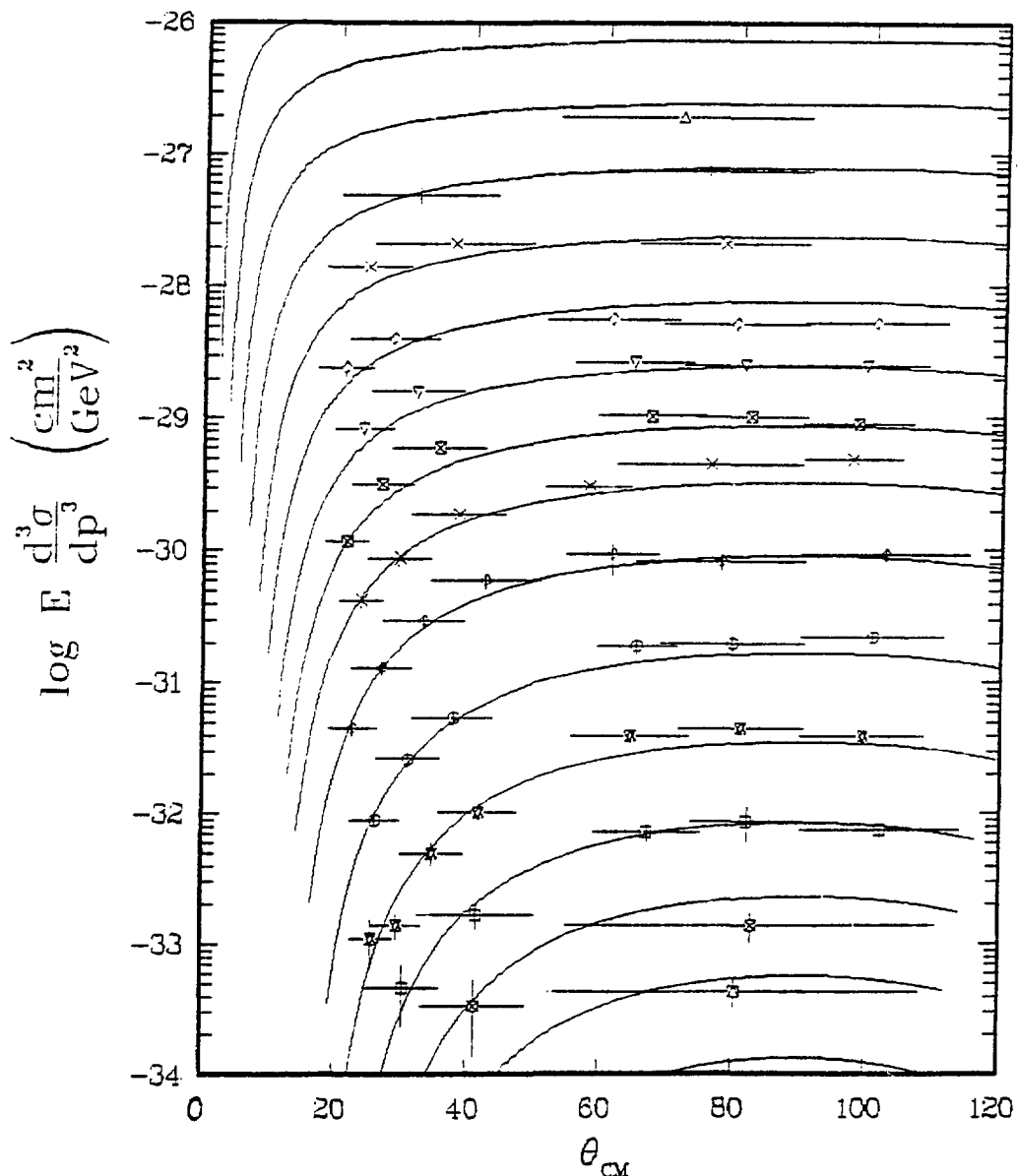


Fig. 14

pp $\rightarrow\pi^{\nu}+X$ @ 300 GeV/c

BNL/CIT/LBL

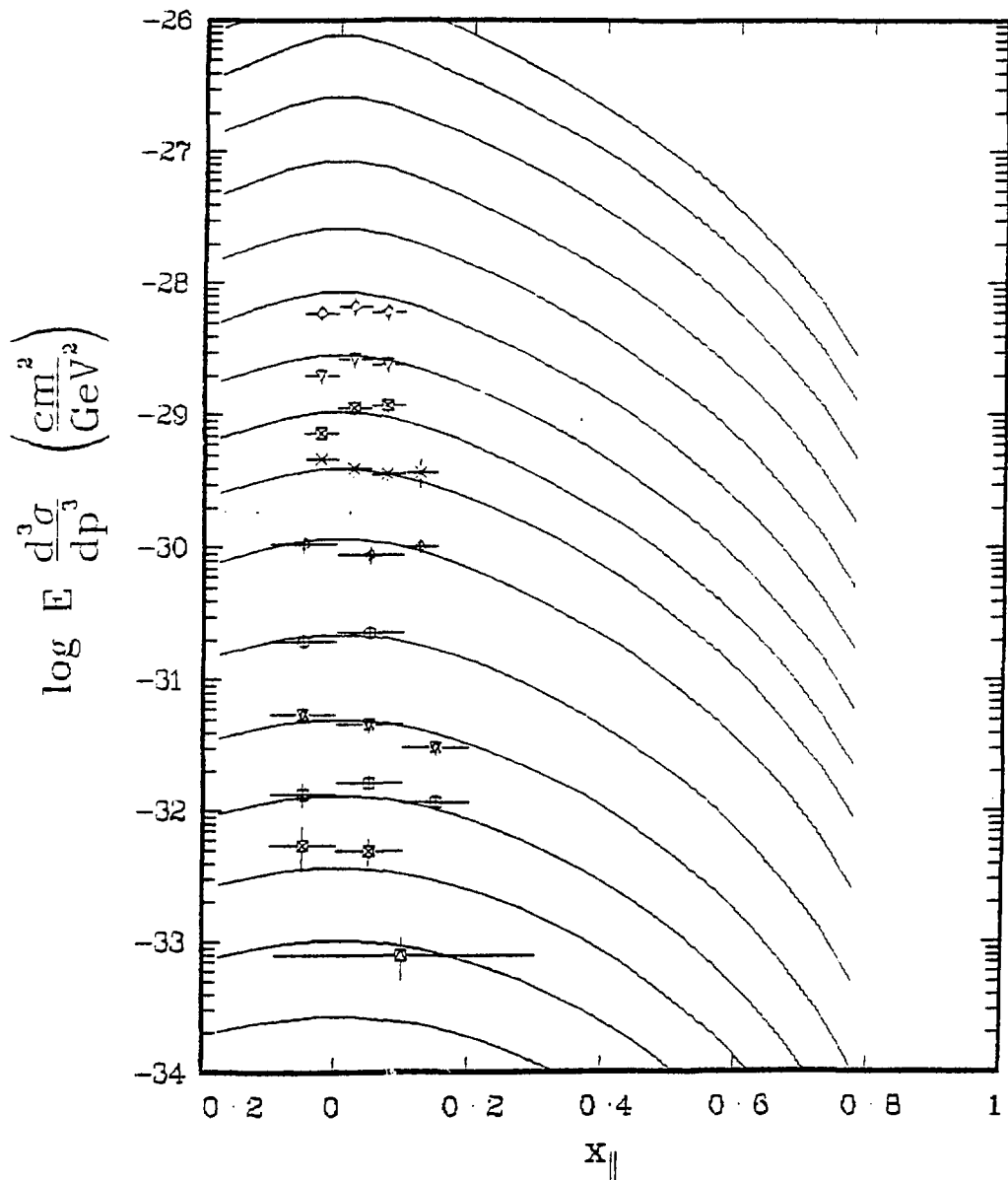


Fig. 15

pp $\rightarrow \pi^0 + X$ @ 300 GeV/c
BNL/CIT/LBL

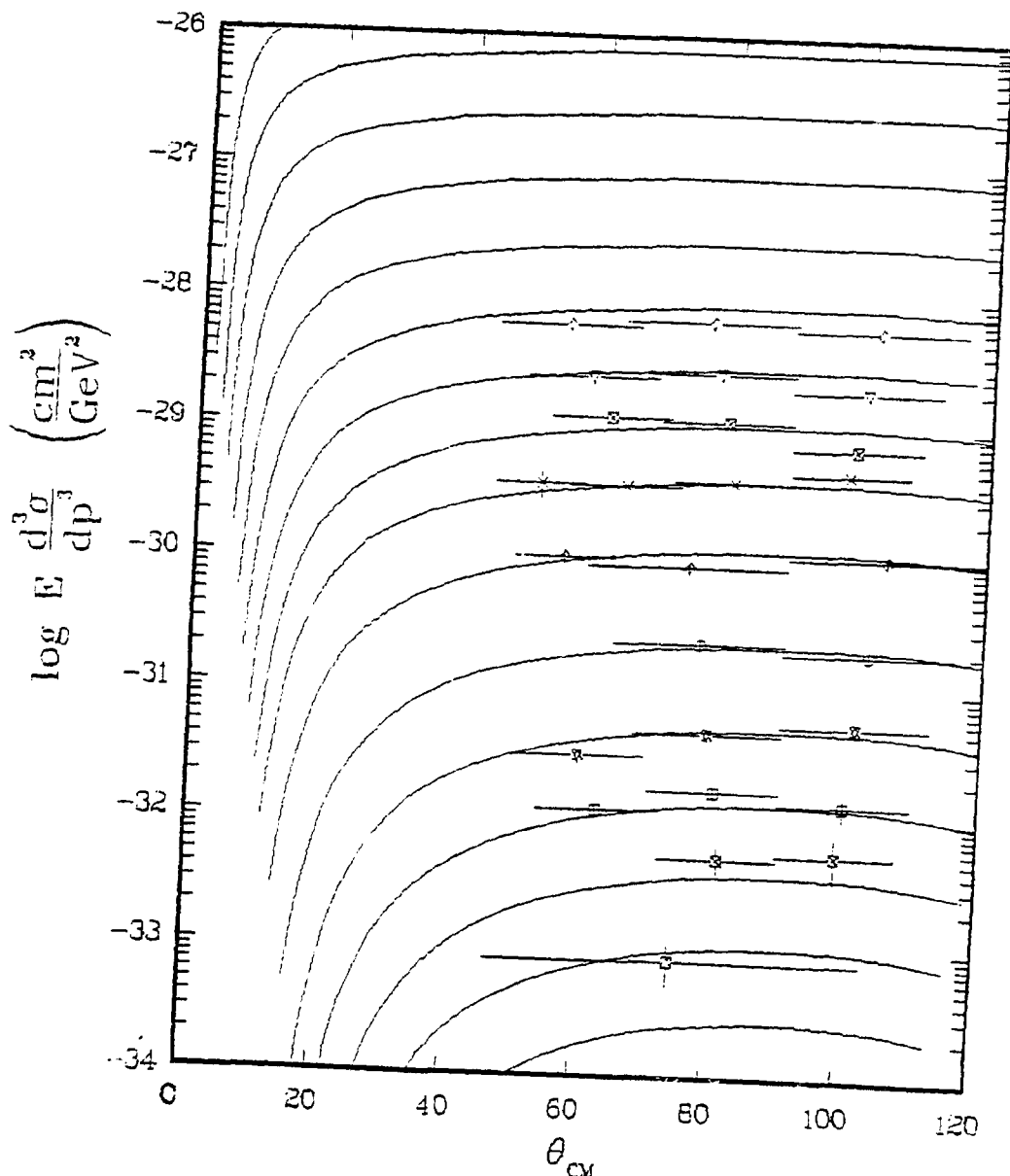


Fig. 16